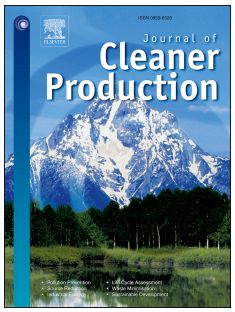

Impacts of climate change on the streamflow of a large river basin in the Australian tropics using optimally selected climate model outputs

Muhammad Usman, Christopher E. Ndehedehe, Humera Farah, Rodrigo Manzanas

PII: S0959-6526(21)02309-X

DOI: https://doi.org/10.1016/j.jclepro.2021.128091

Reference: JCLP 128091

To appear in: *Journal of Cleaner Production*

Received Date: 29 January 2021

Revised Date: 17 May 2021

Accepted Date: 23 June 2021

Please cite this article as: Usman M, Ndehedehe CE, Farah H, Manzanas R, Impacts of climate change on the streamflow of a large river basin in the Australian tropics using optimally selected climate model outputs, *Journal of Cleaner Production* (2021), doi: https://doi.org/10.1016/j.jclepro.2021.128091.

Muhammad Usman. Conceptualization; Muhammad Usman, Christopher E. Ndehedehe, Rodrigo Manzanas. Data curation; Muhammad Usman, Christopher E. Ndehedehe, Rodrigo Manzanas. Formal analysis; Muhammad Usman, Humera Farah, Rodrigo Manzanas. Methodology; Roles/Writing - original draft; Muhammad Usman. Writing - review & editing; Muhammad Usman, Christopher E. Ndehedehe, Humera Farah, Rodrigo Manzanas.

Impacts of climate change on the streamflow of a large river basin in the Australian tropics using optimally selected climate model outputs

Muhammad Usman[1*], Christopher E. Ndehedehe[2], Humera Farah[3], and Rodrigo Manzanas[4]

[1]Pakistan Meteorological Department, Pitras Bukhari Road, H-8/2, Islamabad, Pakistan

[2]Australian Rivers Institute and Griffith School of Environment & Science, Griffith University, Nathan, Queensland 4111, Australia

[3]Department of Earth & Environmental Sciences, Bahria University, Sector E-8, Islamabad, Pakistan

[4]Meteorology Group, Dpto. de Matemática Aplicada y Ciencias de la Computación, Universidad de Cantabria, Santander, 39005, Spain

Corresponding Author: Muhammad Usman (usman666.m@gmail.com)

Impacts of climate change on the streamflow of a large river basin in the Australian tropics using optimally selected climate model outputs

Muhammad Usman[1*], Christopher E. Ndehedehe[2], Humera Farah[3], and Rodrigo Manzanas[4]

[1]Pakistan Meteorological Department, Pitras Bukhari Road, H-8/2, Islamabad, Pakistan

[2]Australian Rivers Institute and Griffith School of Environment & Science, Griffith University, Nathan, Queensland 4111, Australia

[3]Department of Earth & Environmental Sciences, Bahria University, Sector E-8, Islamabad, Pakistan

[4]Meteorology Group, Dpto. de Matemática Aplicada y Ciencias de la Computación, Universidad de Cantabria, Santander, 39005, Spain

Corresponding Author: Muhammad Usman (usman666.m@gmail.com)

Abstract

Climate change affects natural systems, leading to increased acceleration of global water cycle and substantial impacts on the productivity of tropical rivers and the several ecosystem functions they provide. However, the anticipated impacts of climate change in terms of frequency and intensity of extreme events (e.g., droughts and floods) on hydrological systems across regions could be substantially different. This study therefore aims to assess the impacts of climate change on the streamflow of a large river basin located in central Australia (Cooper creek-Bulloo River Basin). Modified version of the hydrological model Hydrologiska Byråns Vattenbalansavdelning (HBV) was used in this study to generate daily streamflow. This model was first calibrated (2001-2010) and then validated for two independent periods (1993-1997 and 2011-2015). The model depicted a good performance in simulating observed streamflow. Climate projection data from multiple general circulation models, including (ACCESS1.0, CanESM2, CESM1-CAM5, CNRM-CM5, GFDL-ESM2M, HadGEM2-CC, MIROC5,

NorESM1-M, ACCESS1-0, ACCESS1-3, CCSM4, CNRM-CM5, CSIRO-Mk3.6, GFDL-CM3, GFDL-ESM2M, HadGEM2, MIROC5, MPI-ESM-LR, and NorESM1-M) in various forms (raw, statistically downscaled, dynamically downscaled, and bias adjusted) were considered in this study. Results showed that three high resolution dynamically downscaled and bias adjusted models (ACCESS1-3, CNRM-CM5, and MPI-ESM-LR) from Terrestrial Ecosystem Research Network (TERN) dataset v1.0.2 have better performance than other models considered, that is, in terms of capturing observed precipitation over the basin. Future climate projections of ensemble of these three models forced with RCP 4.5 and RCP 8.5 emission scenarios were then used to generate streamflow for 2050s (2040-2069) and 2080s (2070-2099). Results of the study indicated that mean annual precipitation was projected to decrease by up to -8% in 2050s and temperature was projected to increase by up to 4.66 °C in 2080s under the average and extreme emission scenarios, respectively. Mean annual, mean seasonal (December-February, March-May, June-August, September-November), and mean monthly streamflow were projected to decrease under different emission scenarios in 2050s and 2080s. These results indicate decreased water availability in the future as well as water cycle intensification. These changes in streamflow might have impacts on agriculture, natural ecosystem, and could lead to water restrictions. The outcome of this study can directly feed into frameworks for sustainable management of water resources and support adaptation strategies that rely on science and policy to improve water resources allocation in the region.

Keywords; Droughts, hydrological impacts, water scarcity, water management, central Australia, TERN dataset version 1.0.2

1. Introduction

Global climate is changing and the vulnerabilities of hydro-ecological, freshwater, and agricultural systems to its impacts are expected to vary across regions due to the contributions of

several atmospheric processes and human actions (Ndehedehe et al., 2021; Zhang et al., 2008; Hailey et al., 2020). Generally, the evidence of climate change impacts on environmental systems, including groundwater variability, surface water, and productivity of wetland ecosystems, among others, is growing (Ndehedehe et al., 2021; Ward et al., 2013; van Dijk et al., 2013). But its impacts on water resources, including key hydrologic metrics such as intensity, frequency, and magnitude will vary substantially at regional and local scales (Troin et al., 2015). As with several other regions, Australia has different and highly variable freshwater habitats and climatic regimes, making it more susceptible to climate change (Head et al., 2014). For instance, the influence of large-scale processes such as the El-Ni˜no-Southern Oscillation on both rainfall and land water storage has been documented (Ndehedehe et al., 2021; Kiem et al., 2016; van Dijk et al., 2013), emphasizing the vulnerability of the region to changes in global climate. Furthermore, Australia has experience more warming from 1910-2011 (0.9°C) (CSIRO 2012) than the global average warming (0.7°C) (Cleugh et al., 2012) and is fast becoming a global climatic hotspot, given the impacts of several multi-scale climatic processes. Most parts of Australia are arid and even more vulnerable to small variations in precipitation, e.g., precipitation deficit in streamflow is up to 2.2 times in east, south, and southwest Australia (Head et al., 2014; van Dijk et al., 2013). These factors and conditions warrant the assessment of region-specific hydrological response to climate change impacts.

Key methodologies used to assess hydrological implications of climate change on water management require the combination of hydrological models with output of General Circulation Models (GCMs), which are based on different climate change scenarios (Luo et al., 2019; Guo et al., 2020; Troin et al., 2015). Notably, hydrological modeling is dependent on accurate information of essential variables such as precipitation. This is because it is considered as a

crucial input for hydrological applications (Masih et al., 2010; Price et al., 2014; Wang et al., 2015; Camici et al., 2018), particularly in arid river basins (Pilgrim et al., 1988). Arguably, the poor skills and large uncertainties of global hydrological and climate models have been linked to limited gauged observations of precipitation and poor representation of surface water balance, among other factors (Ndehedehe, 2019; van Dijk et al., 2014). Reliable information on precipitation inputs is thus crucial to understand streamflow regimes and for accurate estimation of future climate scenarios (Troin et al., 2015; Alnahit et al., 2020).

However, the native resolution of GCMs is considerably coarse, making them more suitable for continental or global scale studies (Di Virgilio et al., 2020). In addition, the use of such models is restricted in region-specific studies or at localized scales (e.g. at a catchment scale). This is because information about climate processes at a finer scale is not provided by the coarse resolution GCMs (Duffy et al., 2003; Li et al., 2010), especially precipitation (Wood et al., 2004). The need for comprehensive catchment-scale assessment of the impacts of climate change on streamflow was recently reported by Eccles et al., (2021). They highlighted the non-linearity of these impacts, emphasizing the need for such assessment to increase preparedness in the advent of future extreme events. Furthermore, different methods have been employed to resolve this scale gap and to transform the climatic patterns simulated at coarser scale to local scale. Statistical downscaling and dynamical downscaling are two widely used approaches for this purpose. In the statistical downscaling, transformation of climate projections from a coarse scale to fine scale is achieved by means of transfer functions (trained) that play the role of connectivity between two spatial resolutions (Li et al., 2010). In dynamical downscaling however, a GCM is driven by a higher-resolution regional climate model (RCM), and the RCM is provided with boundary conditions of GCM gap (Hagemann et al., 2009; Maraun et al., 2010).

A key advantage of statistical downscaling is its lower computational requirement (Li et al., 2010) and dynamical downscaling is considered as an approach that is physically consistent in overcoming the scale gap. As a result of this, and their higher resolution, an improved simulation of climate variables could be achieved (Hagemann et al., 2009; Maraun et al., 2010). Importantly, these methods have benefits and shortcomings and have been comprehensively detailed by Fowler et al., 2007 and Wilby et al., 2009.

This study aims to evaluate the impacts of climate change on the streamflow of a large river basin (Cooper creek-Bulloo River Basin) in Australia. To achieve this, a hydrological model will be calibrated and validated and then will be used for the streamflow projection. Selection of climate model outputs for future hydro-climatological projections is considered as one of the most important and critical step in climate change impact studies. Therefore, different GCMs with varying characteristics will be considered in this study including raw, statistically downscaled, dynamically downscaled, and bias adjusted. Best performing (in term of simulating observed precipitation) models will be selected and ensemble of best performing GCMs will then be used for future hydro-climatological projections. Apart from providing insight to hydrological changes, this study might be useful for management of river ecosystem and water resources in the region. An important outcome of this study is its inherent potential to support adaptation strategies that rely on science and policy to improve water resources allocation.

2. Materials and Methods

2.1. Study area

We consider in this work the Cullyamurra Water Hole station as representative of the Cooper creek-Bulloo River Basin (one of the largest in the state of Queensland), which is located (140.843°E, 27.701°S). The Cooper creek-Bulloo River Basin has a drainage area of 232846 km^2

and a mean elevation of 452 m (Fig. 1). There are more than 10,000 lacustrine/palustrine wetlands in the region. Climatic zones in the basin are desert, grassland, and subtropical. Different wetlands (aquatic ecosystem) including arid and semi-arid lakes, arid swamps, coastal and sub-coastal tree swamps, coastal grass-sedge wetlands, and semi-arid swamps are present in the basin. It is also a home to more than three thousand wildlife species including native, introduced, wetland indicator species, and rare or threatened species (Department of Environment and Science, Queensland, 2016). The basin is dominated by scattered shrubs and grasses, other land cover across the basin consists of mines and quarries, lakes and dams, salt lakes, rain fed cropping, rain fed pasture, wetlands, closed tussock grassland, open hummock grassland, open tussock grassland, dense shrubland, open shrubland, closed forest, open forest, open woodland, woodland, and urban areas (Lymburner et al., 2015) (Fig. 1). Scattered shrubs and grasses are more prominent in low elevation areas in the basin. However, their presence is almost negligible in the northern areas of the basin with high elevation. Open tussock grassland, open woodland, and woodland are more dominant in the areas of higher elevation, and sparsely located in the low to medium elevation areas. The central region of the basin which presents intermediate medium elevation is dominated by open hummock grassland, rain fed cropping, open shrubland, and wetlands. Areas with highest elevation are dominated by woodlands. Six Hydrologic Soil Groups (HSGs) are present in the basin with moderate to high runoff potential i.e. HSG-B, HSG-C, HSG-D, HSG-B/D, HSG-C/D, and HSG-D/D. These HSGs are comprised of different soil texture classes, i.e. sandy load, loamy sand, clay loam, silty clay loam, sandy clay loam, loam, silty loam, silt, clay, silty clay, and sandy clay (Ross et al., 2018).

2.2. Experimental setup

2.2.1. Observed and projected data

On the one hand, observed daily precipitation, temperature, and evapotranspiration data for ninety eight stations in the basin for the period 1986-2015 was extracted from the high resolution (~ 5 km) SILO climate dataset (http://www.longpaddock.qld.gov.au/silo, Jeffrey et al., 2001) and was averaged over the basin. These high-resolution data have been interpolated from the superior quality measurements provided by the Australian Bureau of Meteorology.

On the other hand, several GCMs which provide global future climate projections of different climate variables such as precipitation and temperature were considered for this study. Out of forty different Coupled Model Inter-comparison Project (CMIP5) coarse resolution GCMs, eight GCMs, which presented the best performance over Australia had been identified previously by the Australian government, details can be found in (the interested reader is referred to (CSIRO and BoM, 2015) and (https://www.climatechangeinaustralia.gov.au/en/support-and-guidance/faqs/eight-climate-models-data/ for further details). Description of these eight models is summarized in table SI.

Besides, the eleven CMIP5 GCMs listed in table SII (ACCESS1-0, ACCESS1-3, CCSM4, CNRM-CM5, CSIRO-Mk3.6, GFDL-CM3, GFDL-ESM2M, HadGEM2, MIROC5, MPI-ESM-LR, and NorESM1-M) were selected to be used over Queensland. These models were dynamically downscaled using the Commonwealth Scientific and Industrial Research Organization (CSIRO) regional climate model Conformal Cubic Atmospheric Model (CCAM) for two representative concentration pathways (RCP 4.5 and RCP 8.5), representing average and extreme greenhouse gas emission scenarios (Syktus et al., 2020). The resulting high resolution (~10 km) daily dataset, is called Terrestrial Ecosystem Research Network (TERN) version 1.0.2. In addition, another version of this dataset, which is bias-corrected is also available. These

167 datasets could be accessed from the Queensland Future Climate Dashboard
168 (www.longpaddock.qld.gov.au/qld-future-climate/).

169 *2.2.2. Hydrological model, its setup and development*

170 The Hydrologiska Byråns Vattenbalansavdelning (HBV) model (Bergström 1976;
171 Lindström et al. 1997) is a conceptual hydrological model. A slightly modified version of HBV
172 known as HBV-light (Seibert & Vis 2012) was used in this study to simulate streamflow. It has
173 snow, soil, response, and routing routines. Water flowing through a basin is represented by the
174 model in following ways: Precipitation is first processed by the model with respect to threshold
175 temperature and then it is simulated accordingly. In the next phase, soil routine is employed by
176 the model where precipitation is processed according to the water content of soil box. Then
177 response routine becomes active and groundwater recharge adds up to groundwater box (upper)
178 and percolation is initiated to the groundwater box (lower). Streamflow is then simulated and in
179 the routing routine, transport of generated streamflow is represented along the stream network by
180 the application of a triangular weighing function. HBV-light uses temperature, precipitation, and
181 potential evaporation values as driving variables. For further details on the model, interested
182 readers are referred to (Bergström 1976; Lindström et al. 1997; Seibert & Vis 2012).

183 In order to calibrate the model on a daily time scale, a period of ten years (2001-2010) of
184 data was selected, leaving the year 2000 as spin-up. This particular period was chosen for
185 calibration since it includes different (e.g. nearly normal and extreme) streamflow episodes. For
186 validation, two independent time periods were considered: 1993-1997 and 2011-2015. These two
187 periods were also selected for encompassing different streamflow characteristics. For
188 comprehensiveness, the HBV-light model was calibrated against different objective functions
189 (efficiency metrics). In particular we have used the Nash-Sutcliffe efficiency (NSE); (Nash &

Sutcliffe 1970), Kling Gupta Efficiency (KGE) (Gupta et al., 2009), Lindström measure (Lindström et al. 1997) (hereafter Lm), and Coefficient of determination (R2). These objective functions have a perfect value of 1, i.e. if a value of 1 is achieved for any of these objective functions it will refer to a perfect match between observed and modeled streamflow. The model was calibrated using Genetic Algorithm Protocol (GAP; Seibert 2000) and Powell correction. In order to achieve the best performance in simulating observed streamflow, a two-step calibration procedure was adopted. In the first step the model was calibrated against the four individual objective functions (NSE, KGE, Lm, and R2) by giving a weightage of hundred percent to each of them. In the second step, it was calibrated against different combinations of the four objective functions i.e. NSE+KGE, NSE+Lm, NSE+R2, KGE+Lm, KGE+R2, and R2+Lm by giving a fifty percent weightage to each objective function in each particular combination.

2.2.3. Selection of GCMs for future climate projections

Precipitation is an essential and critical input for hydrological modeling. Since the ability of the different GCMs to reliably reproduce observed precipitation is highly location-dependent (Vaze et al., 2011; Tuo et al., 2016), it is important to select the best performing GCMs for the target region being studied. To this end, five ensembles of different GCMs were considered. The first ensemble consisted of eight GCMs (section 2.2.1) in their raw form (native coarse resolution) and was referred to as AU-GCMs Raw. The second ensemble included the same models but statistically downscaled through bias correction (Delta method) and was referred to as AU-GCMs BC. The third ensemble consisted of the same eight models, but bias corrected with Quantile Mapping method and was referred to as AU-GCMs QM. The fourth ensemble consisted of eleven dynamically downscaled GCMs (section 2.2.1) and was referred to as QLD-

GCMs. Finally, the fifth ensemble of models included these same eleven models but was also bias adjusted other than being dynamically downscaled and was referred to as QLD-GCMs BA.

Performance of these five ensembles to capture observed precipitation was evaluated using several efficiency metrics including, Mean Error (ME), Mean Absolute Error (MAE), Root Mean Square Error (RMSE), Relative Absolute Error (RAE), Relative Volume Error (RVE), Index of Agreement measure (IoAd), KGE, and Percent Bias (PBIAS). Out of the five ensembles the one with the lowest ME, MAE, RMSE, RAE, RVE, PBIAS and highest IoAd and KGE was selected for further analysis. Note that previous studies suggested that GCMs with weak performance should not be included in the final ensemble to be used for future climate projections (see, e.g., Basharin et al. (2016) and Perkins et al. (2007)). Once the selection of the best performing ensemble was done, all the contributing GCMs were individually examined in terms of certain metrics (by giving them a threshold value). Only those models falling within the limits of these (threshold) values were finally selected to form the definitive ensemble. The limits considered for ME were -2 and 2, less than 1.2 for RAE, between -0.1 to 0.1 for RVE, 0.53 for IoAd, above 0.32 for KGE, and between -10 to 10 for PBIAS. The definitive ensemble was built by simply averaging the selected models. Before the use of this ensemble as future climate projections dataset in this study, another comparison (based on mean annual, daily, monthly, 25^{th} percentile, median, and 75^{th} percentile precipitation) was also made between this final ensemble and the initial one, which was selected out of the five ensembles considered. Climate projections from the final ensemble were then used as inputs to the HBV-light model in order to produce streamflow projections for two future periods i.e. 2050s (2040-2069) and 2080s (2070-2099). Note that the methodological approach adopted in this study to select the best performing climate

models is subjective as there is no globally agreed criteria for this task (Smith and Chandler, 2010).

3. Results and Discussion

3.1. Model calibration and validation

The sensitivity of the HBV-light's performance during calibration and validation periods to different objective functions and their combinations was first assessed. The model was calibrated against different objective functions in a way that maximum value (closer to 1) was achieved for each objective function and each combination of objective functions (Section 2.2.2). Values of up to 0.89 and 0.66 were achieved for these objective functions and their combinations during calibration and validation periods respectively. We found out that it does not necessarily mean that higher value of an objective function leads to better performance of the model. For instance, when the model was calibrated against R2 as an objective function, a value of 0.89 was achieved and a value of 0.78 was achieved when the model was calibrated against NSE as an objective function. However, the difference between mean daily observed and modeled streamflow was less in case of NSE, implying a better performance of model in capturing observed streamflow (Fig. 2). In addition it was also found that if a model is calibrated against an objective function or combination of objective functions e.g. R2+Lm and a low difference in observed and modeled streamflow was obtained during calibration period, it does not imply that it will depict the lower difference in observed and modeled streamflow during validation period as well (Fig. 2). Other than the differences in mean daily streamflow (observed vs. modeled) during the calibration period, model's ability to capture extreme streamflow values is also a major factor which has to be considered. Finally it was found out that if a model is calibrated against NSE as an objective function, a good agreement between different characteristics of

streamflow (observed vs. modeled) during calibration and both validation periods was depicted (Fig. 3). These results however are subjective and might be different depending on the region of study and other factors.

3.2. Selection of future climate projections of GCMs

From the results obtained based on the methodology described in section 2.2.3, it was found that AU-GCMs Raw and QLD-GCMs considerably overestimated the mean annual precipitation by up to 41% and 53%, respectively. On the contrary, AU-GCMs BC and AU-GCMs QM substantially underestimated mean annual precipitation by up to 59% and 18%. Finally, QLD-GCMs BA provided the best results with an overestimation of mean annual precipitation by only up to 8%. However, besides PBIAS, several other metrics were employed to further assess the performance of the different ensemble GCMs. Results for all the other metrics, including MAE, ME, RMSE, RAE, RVE, IoAd, and KGE also suggested a better performance of QLD-GCMs BA. At this point, the eleven GCMs conforming the QLD-GCMs BA ensemble were individually evaluated in terms of capturing the historic precipitation based on different threshold values assigned to different metrics (see section 2.2.3). Based on these criteria, three GCMs ACCESS 1-3, CNRM-CM5, and MPI-ESM-LR were selected for the final ensemble, which is referred to as 3QLD-GCMs BA hereafter. Fig. 5 shows that mean monthly precipitation simulated by these three models captures observed precipitation fairly well. Moreover, as shown by Fig. 6, as compared with the total ensemble of eleven GCMs, these three GCMs also exhibit lower difference with respect to observed precipitation beyond mean monthly values.

To the best of our knowledge this is the first time that Queensland climate projection data of 11 GCMs have been evaluated for hydrological applications in comparison with 8 GCMs

selected by Australian Government. This approach could be used in future for the whole state of Queensland and would be beneficial for better understanding of climate change impacts on the streamflow characteristics and water resources management of Queensland's catchments.

3.3. Projected changes in precipitation, temperature, and streamflow

For the assessment of climate change and its associated effects in the hydrology, a baseline period of 1986-2015 was used, and the future changes in precipitation, temperature, and streamflow over CCCWH were computed for 2050s (2040-2069) and (2070-2099) 2080s under the RCP 4.5 and the RCP 8.5 emission scenarios. For simplicity, the period 2050s (2080s) was referred to as the P1 (P2) in the following.

Mean annual precipitation was projected to decrease in P1 by -8% and to decrease only slightly in P2 under the RCP 4.5 emission scenario. Under the RCP 8.5, mean annual precipitation was projected to decrease slightly in P1 and to increase by 6% in P2. Mean annual temperature was projected to increase by 1.95 °C and 2.42 °C in P1and P2 respectively under the RCP 4.5 emission scenario. For the RCP 8.5 emission scenario, mean annual temperature was projected to increase by 2.67 °C and 4.66 °C in P1 and P2, respectively. Mean annual streamflow was projected to decrease by up to -32% in P1 and up to -28% in P2 under the RCP 4.5 emission scenario. Under the RCP 8.5 emission scenario, mean annual streamflow was projected to decrease by up to -31% in P1 and -20% in P2. Overall projected changes in mean annual streamflow were in line with decreasing (increasing) precipitation (temperature) variability under both emission scenarios.

At a seasonal scale, streamflow was projected to decrease by -33% and -27% for DJF in P1 under the RCP 4.5 and RCP 8.5 emission scenarios respectively. A decrease of -24% and -13% was projected for December-January-February (DJF) of P2 under the RCP 4.5 and RCP 8.5

emission scenarios respectively. A decrease of -33% and -43% in streamflow was projected for MAM in P1 under the RCP 4.5 and RCP 8.5 emission scenarios respectively, while streamflow was projected to reduce by -52% and -46% for the same season in P2 under the RCP 4.5 and RCP 8.5 emission scenarios respectively. For June-July-August (JJA) in P1, streamflow was projected to decrease by -16% and -31% under the RCP 4.5 and RCP 8.5 emission scenarios respectively, and a decrease of -26% and -19% was projected for the same season in P1 under the respective emission scenarios. Streamflow was projected to decrease by -29% for September-October-November (SON) in P1 under the RCP 4.5 and RCP 8.5 emission scenarios, and the decrease of -7% and 8% was projected for SON in P2 under the RCP 4.5 and RCP 8.5 emission scenarios respectively.

On a monthly scale, maximum decrease of -76% in July streamflow and a maximum increase of 35% in October streamflow was projected for P1 under the extreme emission scenario i.e. RCP 8.5 (Fig. 7). July streamflow was projected to undergo a maximum decrease of -81% under the RCP 4.5 emission scenario in P2 and an increase of 48% was projected in October streamflow in the same period under the RCP 8.5 emission scenario. Overall mean monthly streamflow was projected to decrease by -29% and -36% in P1 under the RCP 4.5 and RCP 8.5 emission scenarios respectively and mean monthly streamflow was projected to decrease by -33% and -29% in P2 under the RCP 4.5 and RCP 8.5 emission scenarios respectively.

3.4. Discussion

Different sources of uncertainties are attributed to the process of assessing climate change impacts on streamflow characteristics. Large sources of uncertainties are related to the hydrological models and General Circulation Models (GCMs) among others (Vettter et al.,

2017). To reduce hydrological model related uncertainties, the hydrological model setup and development was considered. It is crucial for a hydrological model that is being used for assessing changes in future streamflow, to represent observed streamflow with an acceptable accuracy. The goal here was to calibrate and validate the HBV-light model in such a way that modeled streamflow could show sensitivity to both mean and extreme observed events. To achieve this, we have considered a range of objective functions and their combinations i.e. NSE, KGE, Lm, R2, NSE+KGE, NSE+Lm, NSE+R2, KGE+Lm, KGE+R2, and R2+Lm. The sensitivity of model's performance during calibration and validation periods to these objective functions and their combinations was assessed. Results showed that it does not necessarily mean that if the model is calibrated against an objective function with a higher value, it will be a better representative of observed streamflow. For example, when the model was calibrated against R2 as an objective function, a high value of 0.89 was achieved during the calibration period and a value of 0.78 was achieved for the same period when the model was calibrated against NSE as an objective function. However, the difference between mean daily observed and modeled streamflow was less in case of NSE, implying a better performance of model in capturing observed streamflow (Fig. 2). Additionally,, it was also observed that if a model was calibrated against an objective function or a combination of objective functions e.g., R2+Lm and a low difference in observed and modeled streamflow was obtained during calibration period, it does not imply that it will depict the lower difference in observed and modeled streamflow during all validation periods as well (Fig. 2). For instance, the difference between observed and modeled mean daily streamflow was less when the model was calibrated against R2+Lm during calibration and second validation period, however the difference in observed and modeled streamflow was substantial during first validation period (Fig. 2). Our results also point out the

importance of considering two independent periods for validation. Our aim was to achieve the performance of the model, which was fairly acceptable during calibration and both validation periods. Along with the differences in mean daily streamflow (observed and modeled) during calibration and validation periods, model's ability in capturing other characteristics of observed streamflow e.g. high and low streamflow was also considered. Finally, it was found out that if a model was calibrated against NSE as an objective function, a good agreement between different characteristics of streamflow (observed and modeled) during calibration and both validation periods was achieved (Figs. 3 and 4).

To reduce the uncertainties related to the choice of GCM, this study used 19 different GCMs, namely ACCESS1.0, CanESM2, CESM1-CAM5, CNRM-CM5, GFDL-ESM2M, HadGEM2-CC, MIROC5, NorESM1-M, *ACCESS1-0, ACCESS1-3, CCSM4, CNRM-CM5, CSIRO-Mk3.6, GFDL-CM3, GFDL-ESM2M, HadGEM2, MIROC5, MPI-ESM-LR, and NorESM1-M.* Climate projections from the first eight models were considered in their different forms including raw, as well as statistically downscaled through Delta and Quantile Mapping bias correction methods. The rest of the *models* were considered in their two forms; dynamically downscaled and dynamically downscaled with bias adjustments. To use the projections of a climate model for projecting future streamflow, it is imperative to see how that model replicates the observed precipitation over a recent historical period, since this variable plays a key role in climate change impacts on streamflow studies. After employing multiple statistics, we found that three GCMs (ACCESS1-3, CNRM-CM5, and MPI-ESM-LR), which were dynamically downscaled and subsequently bias adjusted, exhibited a better performance in capturing observed precipitation patterns over our target region (Figs. 4 and 5).

Our study reflects multiple sources of uncertainty that could arise in selection of future climate projections. We have considered raw GCMs, statistically downscaled GCMs, dynamically downscaled GCMs, bias adjusted GCMs. Other than this we employed extensive statistical metrics (Mean Error (ME), Mean Absolute Error (MAE), Root Mean Square Error (RMSE), Relative Absolute Error (RAE), Relative Volume Error (RVE), Index of Agreement measure (IoAd), KGE, and Percent Bias (PBIAS), mean annual, daily, monthly, 25^{th} percentile, median, and 75^{th} percentile modeled and observed precipitation) to measure the models' performance against observed climate data. Our methodology here is not only improved but comprehensive in the sense that we have considered a range of uncertainties and after going through strict assessment, we have finally selected the best performing models that are able to capture observed variability for precipitation, which is a key variable to reliably project streamflow in a hydrological impact study.

Our results indicated an overall decrease in annual precipitation in the P1 and P2 under the RCP 4.5 and RCP 8.5 emission scenarios. However, there was an exception that mean annual precipitation was projected to increase in P2 under the RCP 8.5 emission scenario. Results of this study also indicated an increase in mean annual temperature in P1 and P2 under RCP 4.5 and RCP 8.5 emission scenarios. Mean annual streamflow was also projected to decrease, which is in line with decreasing precipitation and rising temperature. However, streamflow was also projected to decrease in P2 under the RCP 8.5 emission scenario, in which the precipitation was projected to increase. This relationship between climate variables and streamflow might be attributed to different factors. For the said scenario and period an exceptional increase in temperature was also projected. For instance, an increase of 2.42 °C was projected for the same period under the RCP 4.5 emission scenario, however, it was 4.66 °C under the extreme emission

394 scenario. High temperature may lead to more evapotranspiration, resulting in reduced streamflow
395 and net precipitation (water availability). Furthermore, changes in climatic variables such as
396 precipitation have a strong impact on streamflow and are typically amplified in streamflow by
397 few times, and even an insignificant variation of climate variables could lead to substantial
398 changes in streamflow (Chiew et al., 2009; Hattermann et al., 2011; Reshmidevi et al., 2018).
399 Response of streamflow to meteorological conditions, however, is highly nonlinear (Van Dijk et
400 al., 2013) because different climate variables e.g. temperature and precipitation might have
401 opposite impacts on streamflow. In different regions of Australia, a change of 1% in mean
402 annual precipitation might amplify streamflow by up to 3.5% (Chiew, 2006) and in some
403 instances by up to 4.1% (van Dijk et al., 2013). Depending on some regions within Australia
404 (e.g. southwest Western Australia), changes between 0-40% in precipitation could lead to
405 changes in streamflow in the range of 10-80% (Barria et al., 2015). Streamflow is also sensitive
406 to changes in temperature e.g. an increase of up to 1.0 °C in maximum temperature could lead to
407 a change of up to 5% in annual streamflow and this change could be even higher in different
408 seasons in a range of -10 to 50% (Zhang et al., 2019) and a temperature changes between 0 to 3
409 °C could lead to a change of up to 80% in streamflow (Barria et al., 2015).

410 Our results indicated an overall decrease in mean annual, seasonal, and monthly
411 streamflow. Different studies (Charles et al., 2010; Al-Safi & Sarukkalige, 2018) reported
412 decreasing future streamflow trends in different regions of Australia. Our results are in line with
413 these previous findings. Reduced streamflow might trigger drought-like conditions in future and
414 could have adverse environmental and ecological implications. A considerable reduction in
415 projected streamflow e.g. in the (dry period) autumn and winter might result in the loss of
416 resilience as well as the hydrological connectivity (Petrone et al., 2010) and depletion of

groundwater resources. Droughts are key constraints to flow connectivity and disruption of the physical processes that sustains aquatic biodiversity (Ndehedehe et al., 2020; Ward et al., 2013). Projected decrease in streamflow of Cooper Creek-Bulloo River Basin is also an indication towards water scarcity, which might have substantial impacts on agriculture (ABS, 2011), restricted water use, and bushfires (van Dijk et al., 2013). The variability in flow regimes (magnitude, duration, frequency) as well as the timing and rates of change of flow have important implications on the productivity of wetland ecosystems (Ndehedehe et al., 2020). In articulating how this underpin ecosystem services, fish populations, for instance, benefit from increased sustained flows, which helps in facilitating fish migration to more extensive, productive floodplain areas (e.g., (Ndehedehe et al., 2021b; Thompson et al., 2016). This comes with apparent benefits to the ecological communities supported by freshwater habitats and who rely on wetlands that persist from floodplain inundation to generate numerous cultural, recreational and economic values through commercial fisheries and other human uses of these habitats (Ndehedehe et al., 2020). With projected decrease in river flows as shown in this study for the Cooper creek-Bulloo River Basin, declines in the productivity of freshwater habitats and the higher order organisms that depend on them as well as reductions in the opportunities for local communities is likely. Furthermore, while changes in stream flow regimes could be climate driven through frequent droughts caused by large-scale climate variability indices like the ENSO, increasing human water needs for agriculture and domestic use are increasingly exacerbating stream flow reduction and depletion of hydrological stores such as groundwater (Ndehedehe et al., 2021). This is the case in the Murray Darlin Basin (MDB) in Australia where the expansion of irrigated agriculture has been particularly rapid, and the need for surface water is increasing due to both climate change and increasing human needs. Recently, the eco-

hydrological impacts of water infrastructure development in the MDB shows pronounced impacts during dry climatic phases (Karimi et al., 2021). Under a drying climate scenario accompanied by substantial flow alteration, the impact on aquatic ecosystems, including water holes is ultimately inevitable.

4. Conclusions

This study evaluated the impacts of climate change on the streamflow of the Cooper creek-Bulloo River Basin under the two greenhouse gas emission scenarios, namely RCP 4.5 and RCP 8.5. The hydrological model HBV-light was calibrated and validated at a daily time scale in order to accurately project future streamflow. In order to reduce the uncertainties related to the choice of climate model in future streamflow projections, the performance of nineteen different GCMs from the fifth phase of the Global Model Inter-comparison Project (CMIP5) to reproduce precipitation over the target region was assessed. The three-best performing GCMs namely ACCESS1-3, CNRM-CM5, and MPI-ESM-LR were selected to build an ensemble of future precipitation and temperature projections which were used to feed the HBV-light model. Other main findings of this study are detailed in what follows.

Mean annual precipitation (temperature) is projected to decrease (increase) in 2050s and 2080s under both RCP 4.5 and RCP 8.5 emission scenarios. As a result, mean annual streamflow is projected to decrease in both future periods under the two RCPs. More in detail, the highest decrease in streamflow is expected to occur in MAM, with a reduction of up to -44%. Moreover, streamflow peak is expected to shift from February to January in the future.

Reduction in streamflow is an indication for a depletion in water reserves and a decreased water availability in future, which ultimately impacts agricultural activities, reservoir operations, and ecosystem. From a water management perspective, findings from this study (reduction in

future streamflow) might help decision and policy makers in proactive and sustainable water resources management.

Declaration of Competing Interest

The authors declare that they have no known competing financial interests or personal relationships that could have appeared to influence the work reported in this paper.

Funding

This research did not receive any specific grant from funding agencies in the public, commercial, or not-for-profit sectors.

Reference

Alnahit, A.O., Mishra, A.K., & Khan, A.A. (2020). Evaluation of high-resolution satellite products for streamflow and water quality assessment in a Southeastern US watershed. *Journal of Hydrology: Regional Studies, 27*, 100660. https://doi.org/10.1016/j.ejrh.2019.100660.

Al-Safi, H. I. J., & Sarukkalige, P. R. (2018). Evaluation of the impacts of future hydrological changes on the sustainable water resources management of the Richmond River catchment. *Journal of Water and Climate Change, 9*(1), 137-155.

Australian Bureau of Statistics (ABS) (2011), Australian National Accounts, National Income, Expenditure and Product, Cat. Nos. 5204.0 and 5206.0, Australian Bureau of Statistics, Canberra.

Barria, P., Walsh, K.J., Peel, M.C., & Karoly, D. (2015). Uncertainties in runoff projections in southwestern Australian catchments using a global climate model with perturbed physics. *Journal of Hydrology*, *529*, pp.184-199.

Basharin, D., Polonsky, A., & Stankūnavičius, G. (2016). Projected precipitation and air temperature over Europe using a performance-based selection method of CMIP5 GCMs. *Journal of Water and Climate Change, 7*(1), 103-113. https://doi.org/10.2166/wcc.2015.081.

Bergström, S., 1976: Development and Application of a Conceptual Runoff Model for Scandinavian Catchments. Norrköping, 134 pp.

Brown, J. R., Moise, A. F., Colman, R., & Zhang, H. (2016). Will a warmer world mean a wetter or drier Australian monsoon?. *Journal of Climate*, *29*(12), 4577-4596. https://doi.org/10.1175/JCLI-D-15-0695.1.

Camici, S., Ciabatta, L., Massari, C. & Brocca, L. (2018). How reliable are satellite precipitation estimates for driving hydrological models: A verification study over the Mediterranean area. *Journal of Hydrology, 563*, 950–961. https://doi.org/10.1016/j.jhydrol.2018.06.067.

Charles, S., Silberstein, R., Teng, J., Fu, G., Hodgson, G., Gabrovsek, C., Crute, J., Chiew, F., Smith, I., Kirono, D., Bathols, J., Li, L., Yang, A., Donohue, R., Marvanek, S., McVicar, T., Van Niel, T. & Cai, W. (2010). Climate Analyses for south-west Western Australia. A Report to the Australian Government from the CSIRO South-West Western Australia Sustainable Yields Project, CSIRO, Australia

Chiew, F. H. (2006). Estimation of rainfall elasticity of streamflow in Australia. *Hydrological Sciences Journal*, *51*(4), 613-625. https://doi.org/10.1623/hysj.51.4.613.

Chiew, F. H. S., Teng, J., Vaze, J., Post, D. A., Perraud, J. M., Kirono, D. G. C., & Viney, N. R. (2009). Estimating climate change impact on runoff across southeast Australia: Method, results, and implications of the modeling method. *Water Resources Research*, *45*(10). https://doi.org/10.1029/2008WR007338.

Cleugh H, Smith MS, Battaglia M, Graham P, eds. Climate Change: Science and Solutions for Australia. Collingwood: CSIRO Publishing; 2011

CSIRO, Bureau of Meteorology. State of the climate 2012; 2012

CSIRO and Bureau of Meteorology 2015, Climate Change in Australia Information for Australia's Natural Resource Management Regions: Technical Report, CSIRO and Bureau of Meteorology, Australia.

Department of Environment and Science, Queensland (2016) Cooper Creek drainage basin — facts and maps, WetlandInfo website, accessed 12 January 2021. Available at: https://wetlandinfo.des.qld.gov.au/wetlands/facts-maps/basin-cooper-creek

Di Virgilio, G., Evans, J. P., Di Luca, A., Grose, M. R., Round, V., & Thatcher, M. (2020). Realised added value in dynamical downscaling of Australian climate change. *CLIMATE DYNAMICS*, *54*(11-12), 4675-4692. https://doi.org/10.1007/s00382-020-05250-1.

Duffy, P. B., Govindasamy, B., Iorio, J. P., Milovich, J., Sperber, K. R., Taylor, K. E., ... & Thompson, S. L. (2003). High-resolution simulations of global climate, part 1: present climate. *Climate Dynamics*, *21*(5-6), 371-390. https://doi.org/10.1007/s00382-003-0339-z.

Eccles, R., Zhang, H., Hamilton, D., Trancoso, R. et al., (2021). Impacts of climate change on streamflow and floodplain inundation in a coastal subtropical catchment, *Advances in Water Resources, 147*, 103825. https://doi.org/10.1016/j.advwatres.2020.103825.

Fowler, H. J., Blenkinsop, S., & Tebaldi, C. (2007). Linking climate change modelling to impacts studies: recent advances in downscaling techniques for hydrological modelling. *International Journal of Climatology: A Journal of the Royal Meteorological Society*, *27*(12), 1547-1578. https://doi.org/10.1002/joc.1556.

Guo, Y., Fang, G., Xu, Y. P., Tian, X., & Xie, J. (2020). Identifying how future climate and land use/cover changes impact streamflow in Xinanjiang Basin, East China. *Science of The Total Environment*, *710*, 136275. https://doi.org/10.1016/j.scitotenv.2019.136275.

Gupta, H. V., Kling, H., Yilmaz, K. K. & Martinez, G. F. (2009). Decomposition of the mean squared error and NSE performance criteria: Implications for improving hydrological modelling. *Journal of Hydrology*, *377*(1), 80-91. https://doi.org/10.1016/j.jhydrol.2009.08.003.

Haile, G. G., Tang, Q., Leng, G., Jia, G., Wang, J., Cai, D., ... & Zhang, Q. (2020). Long-term spatiotemporal variation of drought patterns over the Greater Horn of Africa. *Science of The Total Environment*, *704*, 135299. https://doi.org/10.1016/j.scitotenv.2019.135299.

Hattermann, F. F., Weiland, M., Huang, S., Krysanova, V., & Kundzewicz, Z. W. (2011). Model-supported impact assessment for the water sector in central Germany under climate change—a case study *Water Resources Management, 25* 3113–34.

Head, L., Adams, M., McGregor, H. V., & Toole, S. (2014). Climate change and Australia. *Wiley Interdisciplinary Reviews: Climate Change*, *5*(2), 175-197. http://dx.doi.org/10.1002/wcc.255.

Jeffrey, S. J., Carter, J. O., Moodie, K. B., & Beswick, A. R. (2001). Using spatial interpolation to construct a comprehensive archive of Australian climate data. *Environmental Modelling & Software*, *16*(4), 309-330. https://doi.org/10.1016/S1364-8152(01)00008-1.

Kiem, A.S., Johnson, F., Westra, S., van Dijk, A., Evans, J.P., O'Donnell, A., Rouillard, A., Barr, C., Tyler, J., Thyer, M., Jakob, D., Woldemeskel, F., Sivakumar, B., & Mehrotra, R. (2016). Natural hazards in Australia: droughts. *Climatic Change, 139* (1), 37–54.

https://doi.org/10.1007/s10584-016-1798-7.

Karimi, S.S., Saintilan, N., Wen, L., Valavi, R. and Cox, J., 2021. The ecohydrological impact of water resource developments through inundation regime analysis of a large semi-arid floodplain. *Journal of Hydrology*, 596, p.126127. https://doi.org/10.1016/j.jhydrol.2021.126127

Li, H., Sheffield, J., & Wood, E. F. (2010). Bias correction of monthly precipitation and temperature fields from Intergovernmental Panel on Climate Change AR4 models using equidistant quantile matching. *Journal of Geophysical Research: Atmospheres*, *115*(D10). https://doi.org/10.1029/2009JD012882.

Lindström, G., Johansson, B., Persson, M., Gardelin, M., & Bergström, S. (1997). Development and test of the distributed HBV-96 hydrological model. *Journal of hydrology*, *201*(1-4), 272-288.https:// doi.org/10.1016/S0022-1694(97)00041-3

Luo, M., Liu, T., Meng, F., Duan, Y., Bao, A., Xing, W., ... & Frankl, A. (2019). Identifying climate change impacts on water resources in Xinjiang, China. *Science of the total environment*, *676*, 613-626. https://doi.org/10.1016/j.scitotenv.2019.04.297.

Lymburner, L., Tan, P., McIntyre, A., Thankappan, M., Sixsmith, J. (2015). Dynamic Land Cover Dataset Version 2.1. Geoscience Australia, Canberra. http://pid.geoscience.gov.au/dataset/ga/83868

Masih, I., Uhlenbrook, S., Maskey, S., & Ahmad, M. D. (2010). Regionalization of a conceptual rainfall–runoff model based on similarity of the flow duration curve: A case study from the semi-arid Karkheh basin, Iran. *Journal of hydrology*, *391*(1-2), 188-201. https://doi.org/10.1016/j.jhydrol.2010.07.018.

Nash, J. E., & Sutcliffe, J. V. (1970). River flow forecasting through conceptual models part I — A discussion of principles. *Journal of Hydrology*, *10*, 282-290. https://doi.org/10.1016/0022-1694(70)90255-6.

Ndehedehe, C.E., Burford, M.A., Stewart-Koster, B., Bunn, S.E., 2020. Satellite-derived changes in floodplain productivity and freshwater habitats in northern Australia (1991–2019). *Ecological Indicators, 114*, 106320. https://doi.org/10.1016/j.ecolind.2020.106320.

Ndehedehe, C. E., Ferreira, V. G., Agutu, N. O., Onojeghuo, A. O., Okwuashi, O., Kassahun, H. T., and Dewan, A. (2021). What if the rains do not come? *Journal of Hydrology, 595*,126040. doi:10.1016/j.jhydrol.2021.126040.

Ndehedehe, C.E., Onojeghuo, A.O, et al., (2021b). Upstream flows drive the productivity of floodplain ecosystems in tropical Queensland, *Ecological Indicators*, 125, 107546. https://doi.org/10.1016/j.ecolind.2021.107546.

Ndehedehe, C.E. (2019). The water resources of tropical West Africa: problems, progress, and prospects. *Acta Geophys, 67*, 621–649 (2019). https://doi.org/10.1007/s11600-019-00260-y.

Nicholls, N., Drosdowsky, W., & Lavery, B. (1997). Australian rainfall variability and change. *Weather*, *52*(3), 66-72. https://doi.org/10.1002/j.1477-8696.1997.tb06274.x.

Perkins, S. E., Pitman, A. J., Holbrook, N. J., & McAneney, J. (2007). Evaluation of the AR4 climate models' simulated daily maximum temperature, minimum temperature, and precipitation over Australia using probability density functions. *Journal of climate*, *20*(17), 4356-4376. https://doi.org/10.1175/JCLI4253.1.

Petrone, K. C., Hughes, J. D., Van Niel, T. G., & Silberstein, R. P. (2010). Streamflow decline in southwestern Australia, 1950–2008. *Geophysical Research Letters*, *37*(11). https://doi.org/10.1029/2010GL043102.

Pilgrim, D. H., Chapman, T. G., & Doran, D. G. (1988). Problems of rainfall-runoff modelling in arid and semiarid regions. *Hydrological Sciences Journal*, *33*(4), 379-400., DOI: 10.1080/02626668809491261.

Price, K., Purucker, S. T., Kraemer, S. R., Babendreier, J. E., & Knightes, C. D. (2014). Comparison of radar and gauge precipitation data in watershed models across varying spatial and temporal scales. *Hydrological Processes*, *28*(9), 3505-3520. https://doi.org/10.1002/hyp.9890.

Reshmidevi, T. V., Kumar, D. N., Mehrotra, R., & Sharma, A. (2018). Estimation of the climate change impact on a catchment water balance using an ensemble of GCMs. *Journal of Hydrology, 556*, 1192-1204. https://doi.org/10.1016/j.jhydrol.2017.02.016

Ross, C. W., Prihodko, L., Anchang, J. Y., KUMAR, S., Ji, W., & Hanan, N. P. (2018). Global Hydrologic Soil Groups (HYSOGs250m) for Curve Number-Based Runoff Modeling. ORNL DAAC. https://doi.org/10.3334/ORNLDAAC/1566.

Seibert, J., (2000). Multi-criteria calibration of a conceptual runoff model using a genetic algorithm. *Hydrology Earth System Sci*ence, *4*, 215–224, https://doi.org/10.5194/hess-4-215-2000.

Seibert, J., & Vis, M. J. P. (2012). Teaching hydrological modeling with a user-friendly catchment-runoff-model software package. *Hydrology Earth System Science, 16*, 3315–3325, https://doi.org/10.5194/ hess-16-3315-2012.

Smith, I., & Chandler, E. (2010). Refining rainfall projections for the Murray Darling Basin of south-east Australia—the effect of sampling model results based on performance. *Climatic Change*, *102*(3-4), 377-393. https://doi.org/10.1007/s10584-009-9757-1.

Syktus,J., Toombs,N., Wong,K., Trancoso,R., Ahrens,D. (2020): Queensland Future Climate Dataset – Downscaled CMIP5 climate projections for RCP8.5 and RCP4.5. Version 1.0.2. Terrestrial Ecosystem Research Network (TERN). dataset. https://doi.org/10.25901/5e3ba30f141b7

Thompson, J. R., Crawley, A., & Kingston, D. G. (2016). GCM-related uncertainty for river flows and inundation under climate change: the Inner Niger Delta. *Hydrological Sciences Journal*, *61*(13), 2325-2347. DOI: 10.1080/02626667.2015.1117173.

Troin, M., Caya, D., Velázquez, J. A., & Brissette, F. (2015). Hydrological response to dynamical downscaling of climate model outputs: A case study for western and eastern snowmelt-dominated Canada catchments. *Journal of Hydrology: Regional Studies*, *4*, 595-610. https://doi.org/10.1016/j.ejrh.2015.09.003.

Tuo, Y., Duan, Z., Disse, M., & Chiogna, G. (2016). Evaluation of precipitation input for SWAT modeling in Alpine catchment: A case study in the Adige river basin (Italy). *Science of the total environment*, *573*, 66-82. https://doi.org/10.1016/j.scitotenv.2016.08.034.

Van Dijk, A. I., Beck, H. E., Crosbie, R. S., de Jeu, R. A., Liu, Y. Y., Podger, G. M., ... & Viney, N. R. (2013). The Millennium Drought in southeast Australia (2001–2009): Natural and human causes and implications for water resources, ecosystems, economy, and society. *Water Resources Research*, *49*(2), 1040-1057. https://doi.org/10.1002/wrcr.20123.

Van Dijk, A. I. J. M., and L. J. Renzullo (2009), The Australian Water Resources Assessment system: Blending water cycle observations and models at local and continental scale, paper presented at GEWEXiLeaps, Melbourne. http://hdl.handle.net/102.100.100/112808?index=1.

van Dijk, A. I. J. M., Renzullo, L. J., Wada, Y., and Tregoning, P.: A global water cycle reanalysis (2003–2012) merging satellite gravimetry and altimetry observations with a hydrological multi-model ensemble. *Hydrology Earth System Science, 18*, 2955–2973, https://doi.org/10.5194/hess-18-2955-2014, 2014.

Vaze, J., Post, D. A., Chiew, F. H. S., Perraud, J. M., Teng, J., & Viney, N. R. (2011). Conceptual rainfall–runoff model performance with different spatial rainfall inputs. *Journal of Hydrometeorology, 12*(5), 1100-1112. https://doi.org/10.1175/2011JHM1340.1.

Vetter, T., Reinhardt, J., Flörke, M., van Griensven, A., Hattermann, F., Huang, S., ... & Krysanova, V. (2017). Evaluation of sources of uncertainty in projected hydrological changes under climate change in 12 large-scale river basins. *Climatic Change, 141*(3), 419-433. https://doi.org/10.1007/s10584-016-1794-y

Wang, G., Zhang, J., Pagano, T. C., Xu, Y., Bao, Z., Liu, Y., ... & Wan, S. (2016). Simulating the hydrological responses to climate change of the Xiang River basin, China. *Theoretical and Applied Climatology, 124*(3-4), 769-779. https://doi.org/10.1007/s00704-015-1467-1.

Wang, S., Liu, S., Mo, X., Peng, B., Qiu, J., Li, M., Liu, C., Wang, Z., & Bauer-Gottwein, P. (2015). Evaluation of Remotely Sensed Precipitation and Its Performance for Streamflow Simulations in Basins of the Southeast Tibetan Plateau, *Journal of Hydrometeorology, 16*(6), 2577-2594. https://doi.org/10.1175/JHM-D-14-0166.1.

Ward, D.P., Hamilton, S.K., Jardine, T.D., Pettit, N.E., Tews, E.K., Olley, J.M., Bunn, S.E., 2013. Assessing the seasonal dynamics of inundation, turbidity, and aquatic vegetation in the australian wet-dry tropics using optical remote sensing. *Ecohydrology 6* (2), 312–323. https://doi.org/10.1002/eco.1270.

Wilby, R. L., Troni, J., Biot, Y., Tedd, L., Hewitson, B. C., Smith, D. M., & Sutton, R. T. (2009). A review of climate risk information for adaptation and development planning. *International Journal of Climatology: A Journal of the Royal Meteorological Society*, *29*(9), 1193-1215. https://doi.org/10.1002/joc.1839.

Wood, A. W., Leung, L. R., Sridhar, V., & Lettenmaier, D. P. (2004). Hydrologic implications of dynamical and statistical approaches to downscaling climate model outputs. *Climatic change*, *62*(1-3), 189-216. https://doi.org/10.1023/B:CLIM.0000013685.99609.9e.

Zhang, H., Wang, B., Li Liu, D., Zhang, M., Feng, P., Cheng, L., ... & Eamus, D. (2019). Impacts of future climate change on water resource availability of eastern Australia: A case study of the Manning River basin. *Journal of hydrology*, *573*, 49-59. https://doi.org/10.1016/j.jhydrol.2019.03.067.

Zhang, Q., Xu, C. Y., Zhang, Z., Ren, G., & Chen, Y. D. (2008). Climate change or variability? The case of Yellow river as indicated by extreme maximum and minimum air temperature during 1960–2004. *Theoretical and applied climatology*, *93*(1-2), 35-43. https://doi.org/10.1007/s00704-007-0328-y.

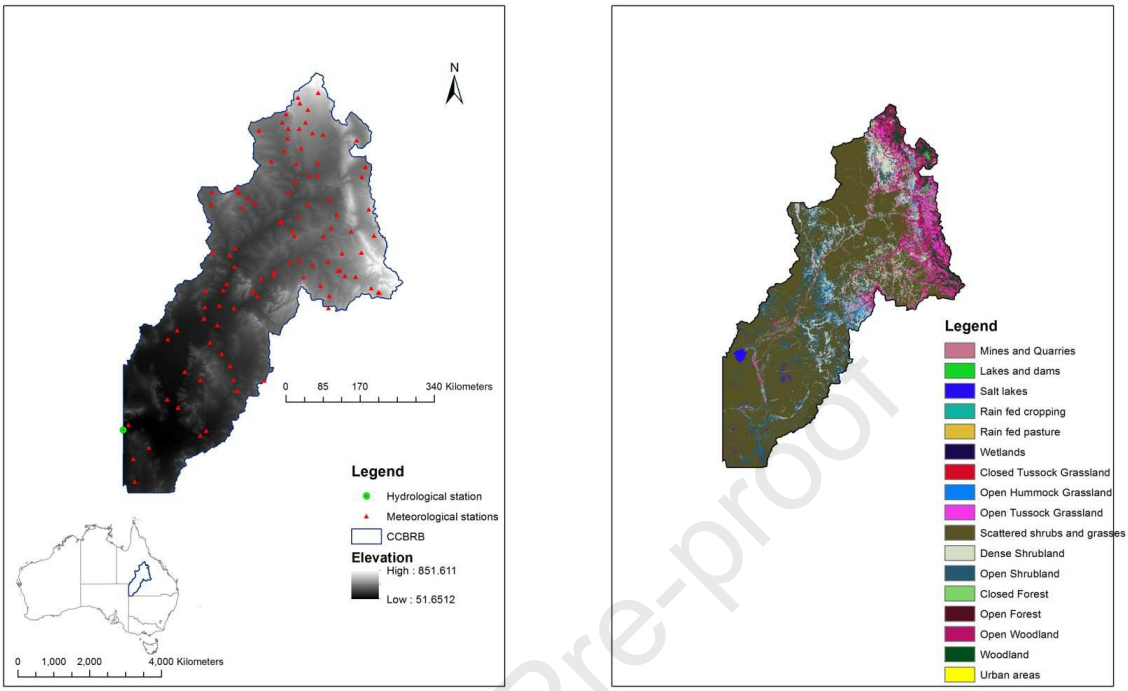

677

678 Figure 1. (Left) Hydro-meteorological stations considered along the target basin. (Right): Land
679 cover.

680

681

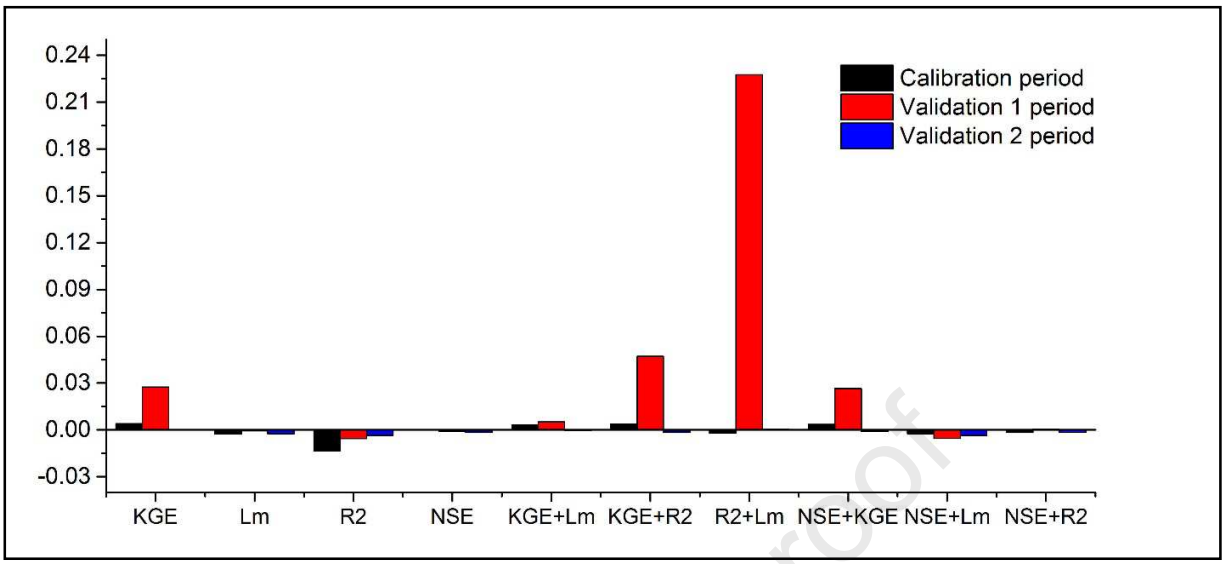

682

683 Figure 2. Differences between mean daily streamflow in mm (observed and simulated) with
684 hydrological model being calibrated and validated against different objective functions and their
685 combinations. Calibration period is from 2001-2010, Validation 1 period is from 1993-1997, and
686 validation 2 period is from 2011-2015.

687

688 Figure 3. Observed and simulated mean daily streamflow during (a) calibration period (b)
689 validation 1 period (c) validation 2 period.

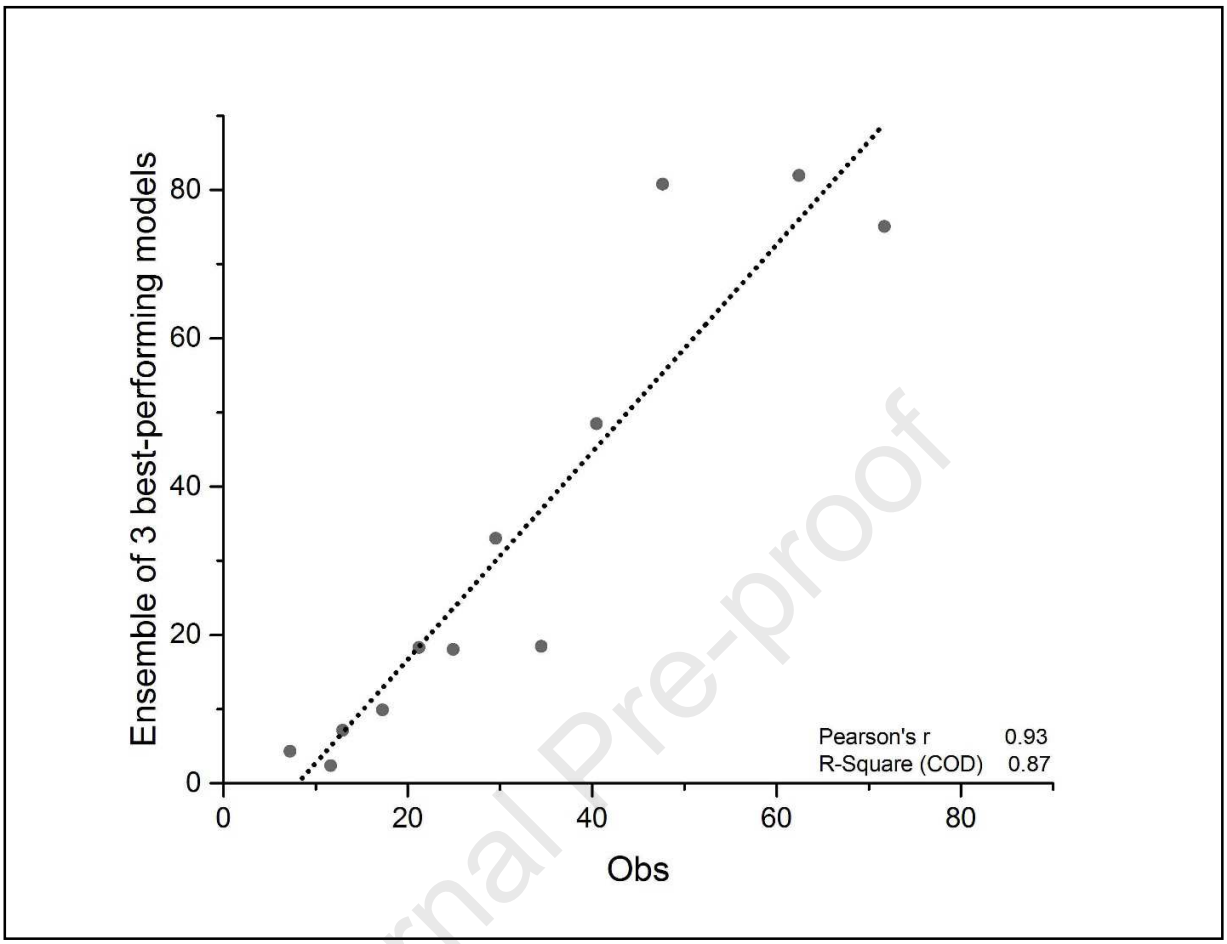

690

691 Figure 4. Long term mean monthly precipitation (mm/month), observed (x-axis) and modeled
692 with ensemble of 3 best-perfroming GCMs (y-axis).

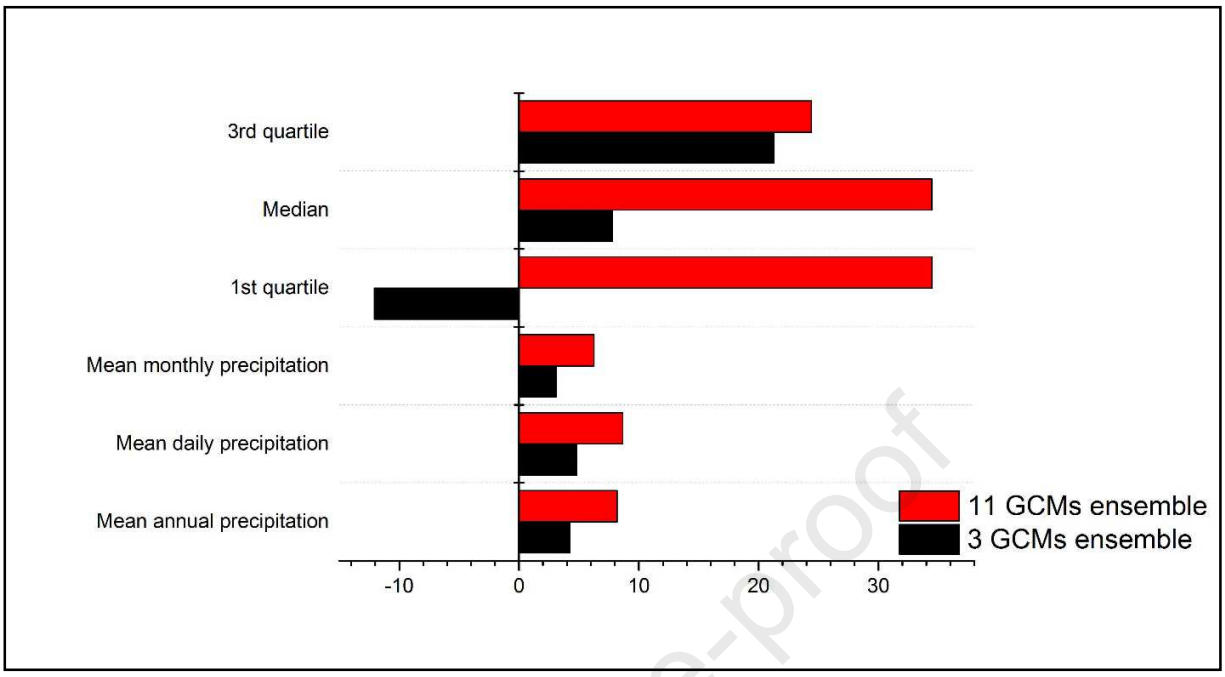

693

694 Figure 5. Performance of finally selected ensemble of 3 GCMs as compared to the ensemble of
695 eleven GCMs in capturing different characteristics of observed precipitation (unit is mm).

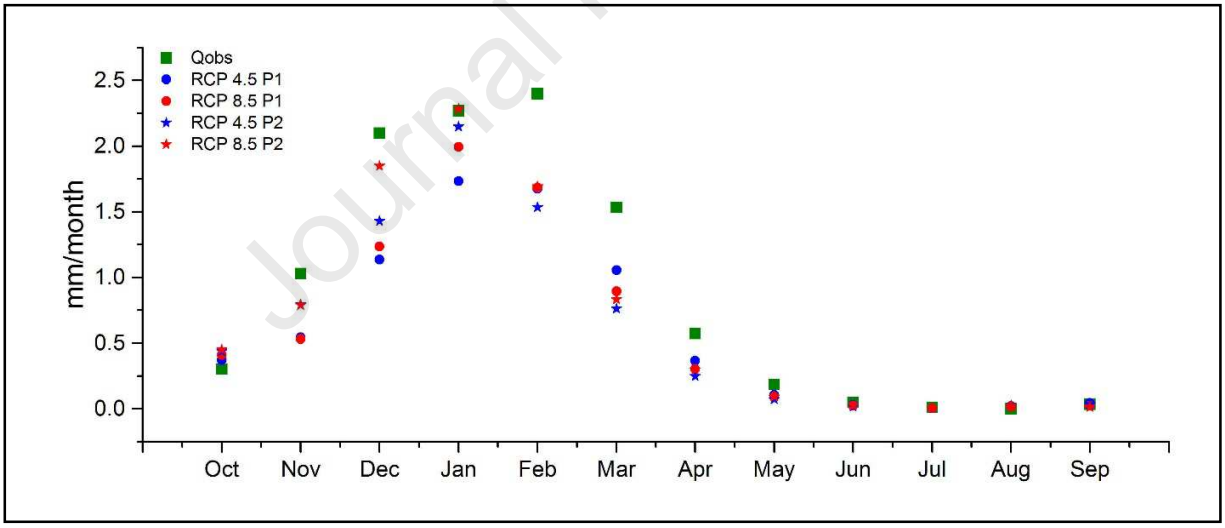

696

697 Figure 6. Projected mean monthly streamflow under the RCP 4.5 and RCP 8.5 emission
698 scenarios for 2040-2069 and 2070-2099 (P1 and P2 respectively), as compared to the historical
699 observed values for the period (1986-2015).

700

701

702 Table SI. Eight CMIP5 GCMs for climate projections for Australia.

Model	Institute, Country	Atmosphere resolution (°)
ACCESS1.0	CSIRO-BOM, Australia	1.9×1.2
CanESM2	CCCMA, Canada	2.8×2.8
CESM1-CAM5	NSF-DOE-NCAR, USA	1.2×0.
CNRM-CM5	CNRM-CERFACS, France	1.4×1.4
GFDL-ESM2M	NOAA, GFDL, USA	2.5×2.0
HadGEM2-CC	MOHC, UK	1.9×1.2
MIROC5	JAMSTEC, Japan	1.4×1.4
NorESM1-M	NCC, Norway	2.5×1.9

703

704 Table SII. Eleven CMIP5 GCMs for climate projections for Queensland.

Model	Institute, Country	Atmosphere resolution (°)
ACCESS1-0	CSIRO & BoM, Australia	1.9×1.2
ACCESS1-3	CSIRO & BoM, Australia	1.9×1.2
CCSM4	NCAR, USA	1.25×0.9424
CNRM-CM5	CNRM & CERFACS, France	1.4×1.4
CSIRO-Mk3.6	CSIRO & Qld Govt, Australia	1.875×1.8653
GFDL-CM3	GFDL NOAA, USA	2.5×2.0
GFDL-ESM2M	GFDL NOAA, USA	2.5×2.0
HadGEM2	MOHC, UK	1.9×1.2
MIROC5	AORI Japan, Japan	1.4×1.4
MPI-ESM-LR	Max Planck Institute, Germany	1.875×1.8653
NorESM1-M	NCC, Norway	2.5×1.9

705

706

Declaration of Competing Interest

The authors declare that they have no known competing financial interests or personal relationships that could have appeared to influence the work reported in this paper.